Influence of genetic mutations to atria vulnerability to atrial fibrillation: an in-silico 3D human atria study

Rebecca Belletti[1], Joaquín Osca[2], Lucia Romero Perez[1], Javier Saiz[1]

[1] Centro de Investigación e Innovación en Bioingeniería, Universitat Politécnica de València, Camino de Vera, s/n, 46022, València, Spain

[2] Electrophysiology Section, Cardiology Department, Hospital Universitari i Politecnic La Fe, Avinguda de Fernando Abril Martorell, 106, Quatre Carreres, 46026, València, Spain

Supplementary Materials

1 3D atrial geometry definition

The 3-dimensional human atrial geometry used in this study was obtained through the segmentation of the atrial anatomical structures from CT scans of a former AF patient; such data were provided by the Hospital Politécnico y Universitario La Fe.

For this purpose, the software Seg3D was employed for automatic volume segmentation, manual adjustments and image processing. Once segmented, the rough surface model was smoothened using a combination of filters provided by the software Paraview and Blender. Subsequently, valve openings and atrial connections were cut and added to the surface model. At this point, atria wall thickness was applied by shrinking the final surface mesh (representing the epicardium), thus obtaining the endocardium, and joining them by closing the contours of the outer and inner surfaces.

The heterogeneity of the atria in terms of electrical properties and conductivity were reflected into the atrial geometry by dividing the model into 21 regions and 53 subregions, as in Ferrer et al [1]. To do so, a semi automatic algorithm was developed in Matlab, based on previous works [2]. The volume mesh was finally obtained by filling the surface model with irregular hexahedral finite elements and by using the software MeshGems for the creation of 3D finite element mesh.

Finally, the ionic model and materials were assigned to the above defined regions using a Matlab algorithm, while fibre orientations were replicated from a previous study [1], since histological data were not available for such patient.

2 Sinus rhythm activation times

The atrial model was stabilized by pacing the SAN region with 5 stimuli at a basic cycle length (BCL) of 1000 ms, so that the electrical differences among the nine electrophysiological regions smoothened. The conduction velocities of the eleven types of tissue were defined by adjusting the longitudinal conductivities (σ_L) and anisotropy ratios ($AR = \sigma_T/\sigma_L$) in order to get a propagation pattern matching the healthy activation sequence experimentally observed [3]. Further refining was needed to avoid propagation blocks due to the funnel effect. The propagation of the electrical wave across the atrial mesh is shown together with the activation times in Figure S1 in healthy conditions, in Figure S2 in presence of the mutation KCNH2 T436M, in Figure S3 in presence of the mutation KCNH2 T895M and in Figure S4 in presence of the mutation KCNE3-V17M. Moreover, in Table S1 the values of the σ_L and AR used in this study are presented.

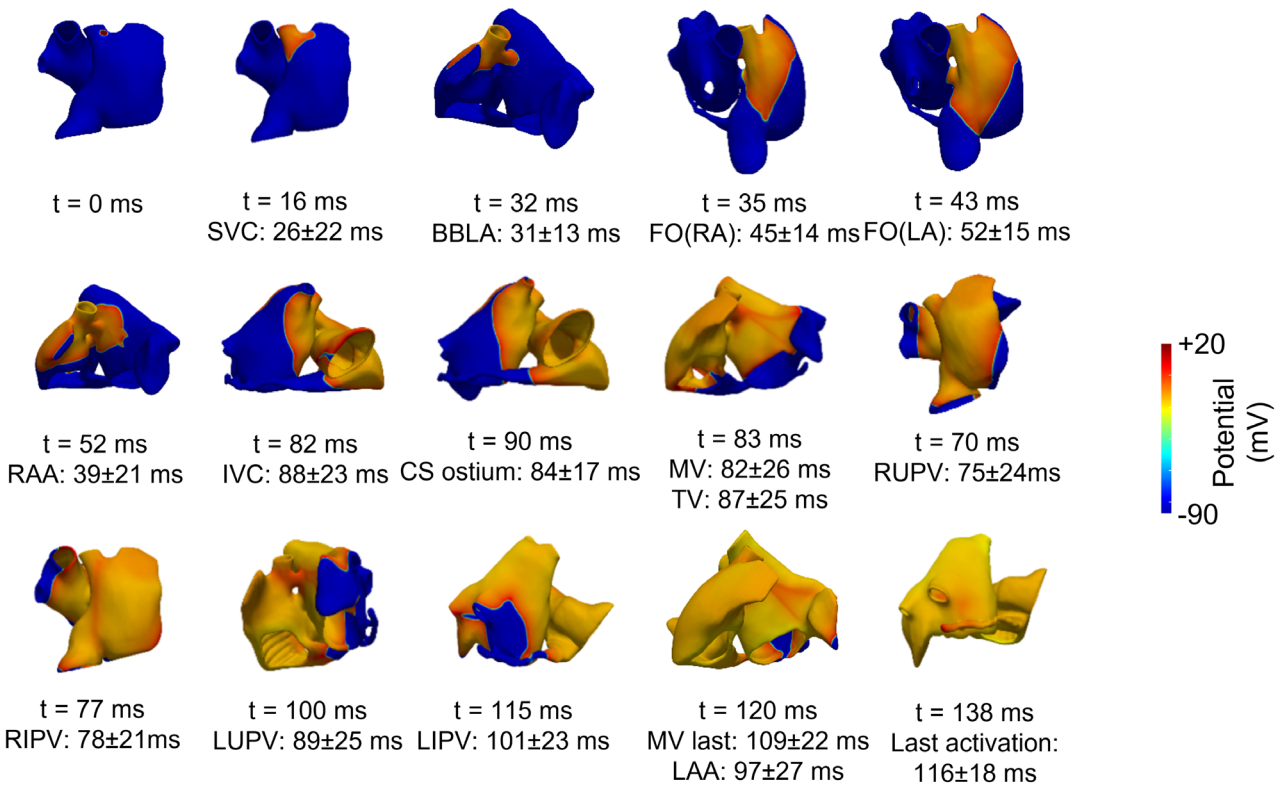

Figure S1 – **Activation times of the atria in WT.** Snapshot of the depolarization wave propagation starting in the SAN with local activation times (ms) in Wild-Type and the corresponding experimental activation range as in [3]. Membrane potential (mV) is color-coded from blue (-90 mV) to red (+20 mV).

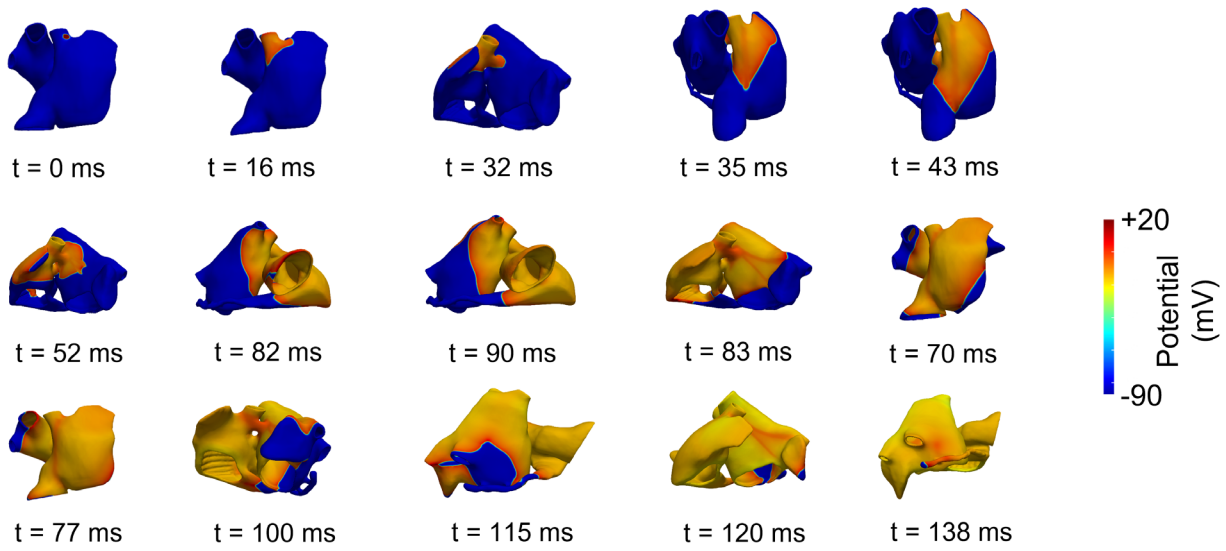

Figure S2 – Activation times of the atria for the mutation KCNH2 T436M. Snapshot of the depolarization wave propagation starting in the SAN with local activation times (ms) in presence of the mutation KCNH2 T436M

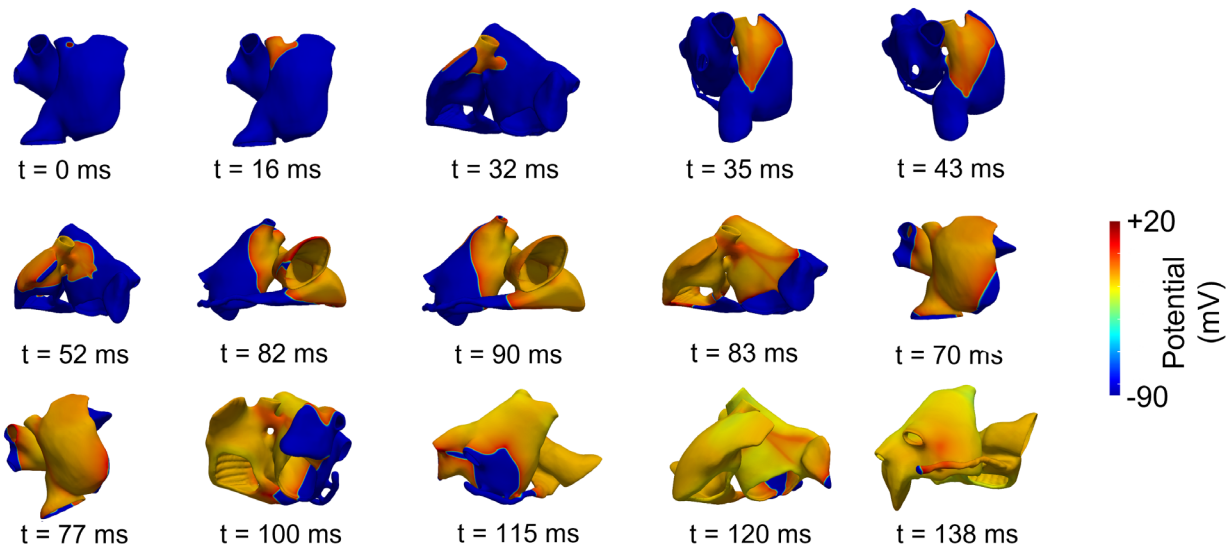

Figure S3 – Activation times of the atria for the mutation KCNH2 T895M. Snapshot of the depolarization wave propagation starting in the SAN with local activation times (ms) in presence of the mutation KCNH2 T895M

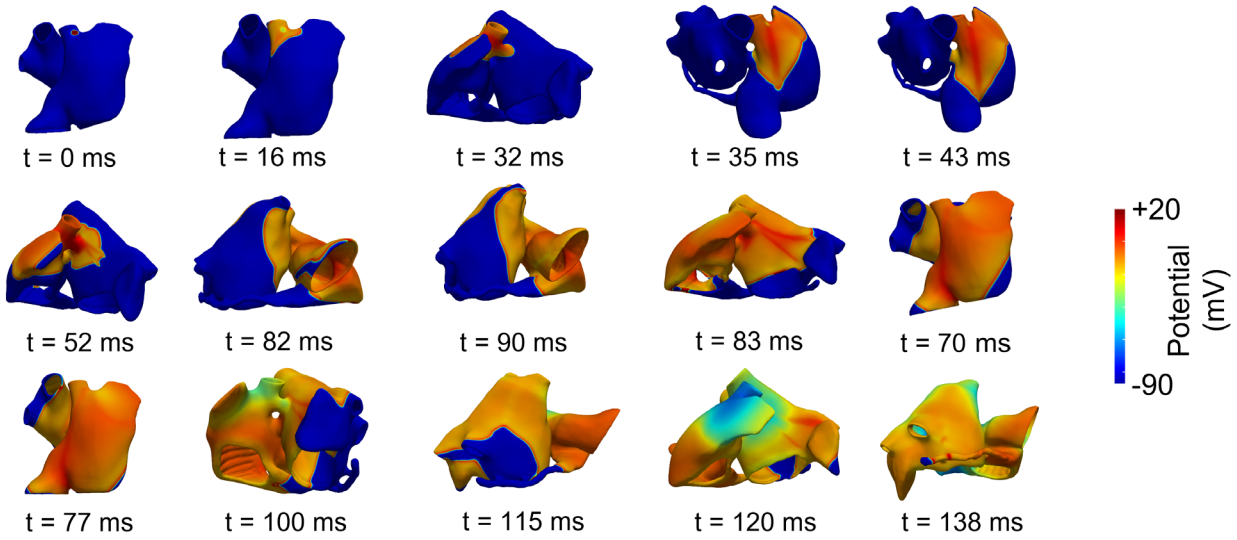

Figure S4 – Activation times of the atria for the mutation KCNE3-V17M. Snapshot of the depolarization wave propagation starting in the SAN with local activation times (ms) in presence of the mutation KCNE3-V17M.

Table S1 - Longitudinal conductivity σ_L (S / cm·pF) and anisotropy ratio AR = σ_T/σ_L for each atrial region in the 3D atrial model.

Region	σ_L	AR = σ_T / σ_L	Region	σ_L	AR = σ_T / σ_L
RA / LA	0.00582	0.35	**SAN**	0.000936	1.00
CT	0.0144	0.15	**FO**	0	1.00

PV	0.003552	0.5	**CS**	0.006	0.5
PM / BBRA	0.00744	0.15	**RFO (FO ring)**	0.00828	0.15
ISTHMUS	0.00144	1.00	**BBLA / FO union**	0.0066	0.15

2.1 Arrhythmia evolution

After stabilizing the atrial model applying 5 beats to the SAN region with BCL set of 1000 ms, an S1-S2 stimulation protocol was applied in sixteen EF locations using two BCLs and eleven CIs to induce AF, as described in paragraph 2.4 and shown in Figure 2A and 2B of the main manuscript. Three examples of the outcomes are shown in Figure S5, S6 and S7.

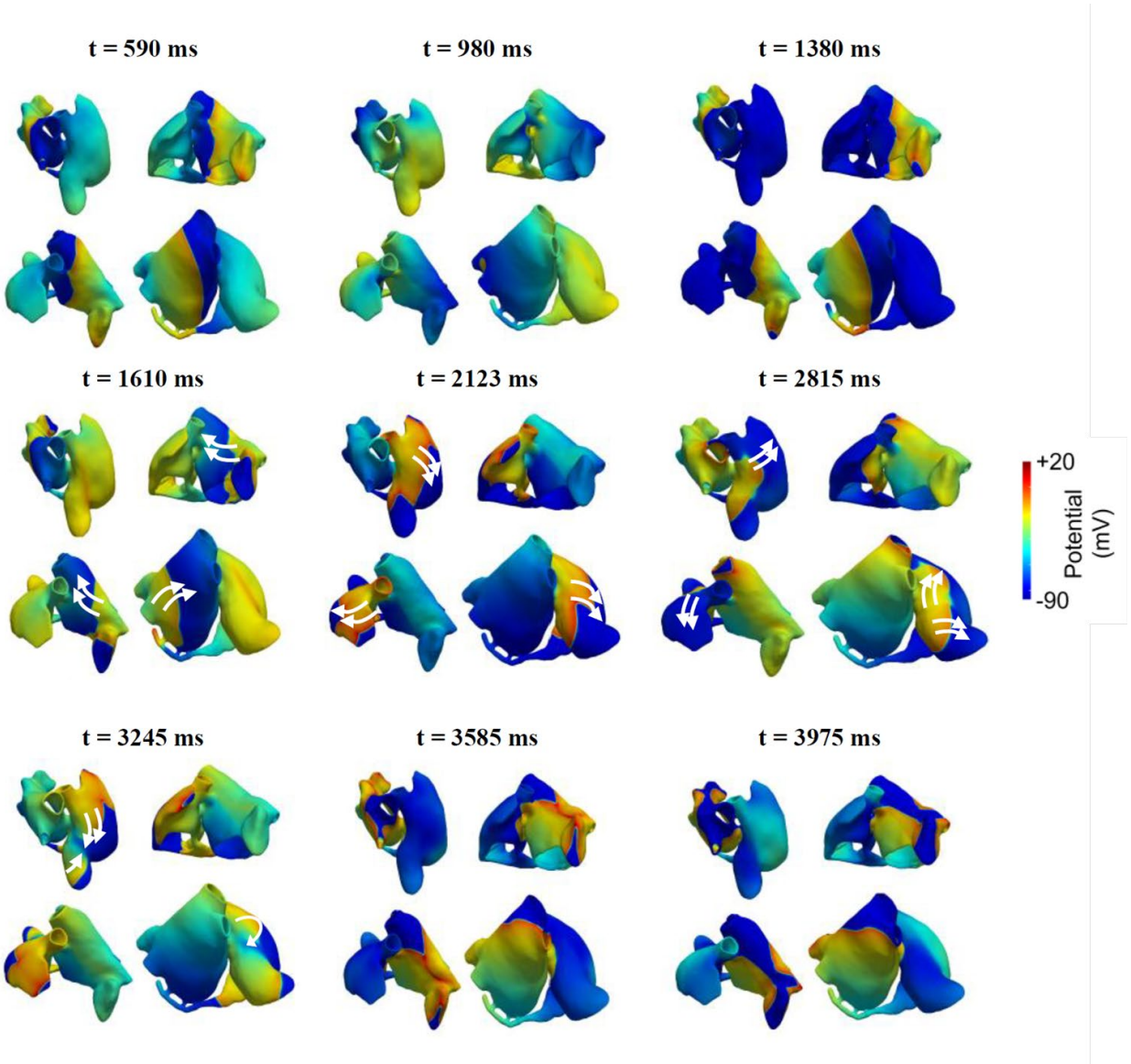

Figure S5 – Snapshot of scroll waves for the mutation KCNH2 T436M. Snapshot of spiral wave activity observed in the 3D patient-specific atrial model in presence of the mutation KCNH2 T436M. The arrhythmic pattern was evoked by stimulating the EF located in the middle of the LPVs, with a BCL equal to 160 ms and with a coupling interval equal to 0 ms. White arrows indicate the direction of the propagating waves.

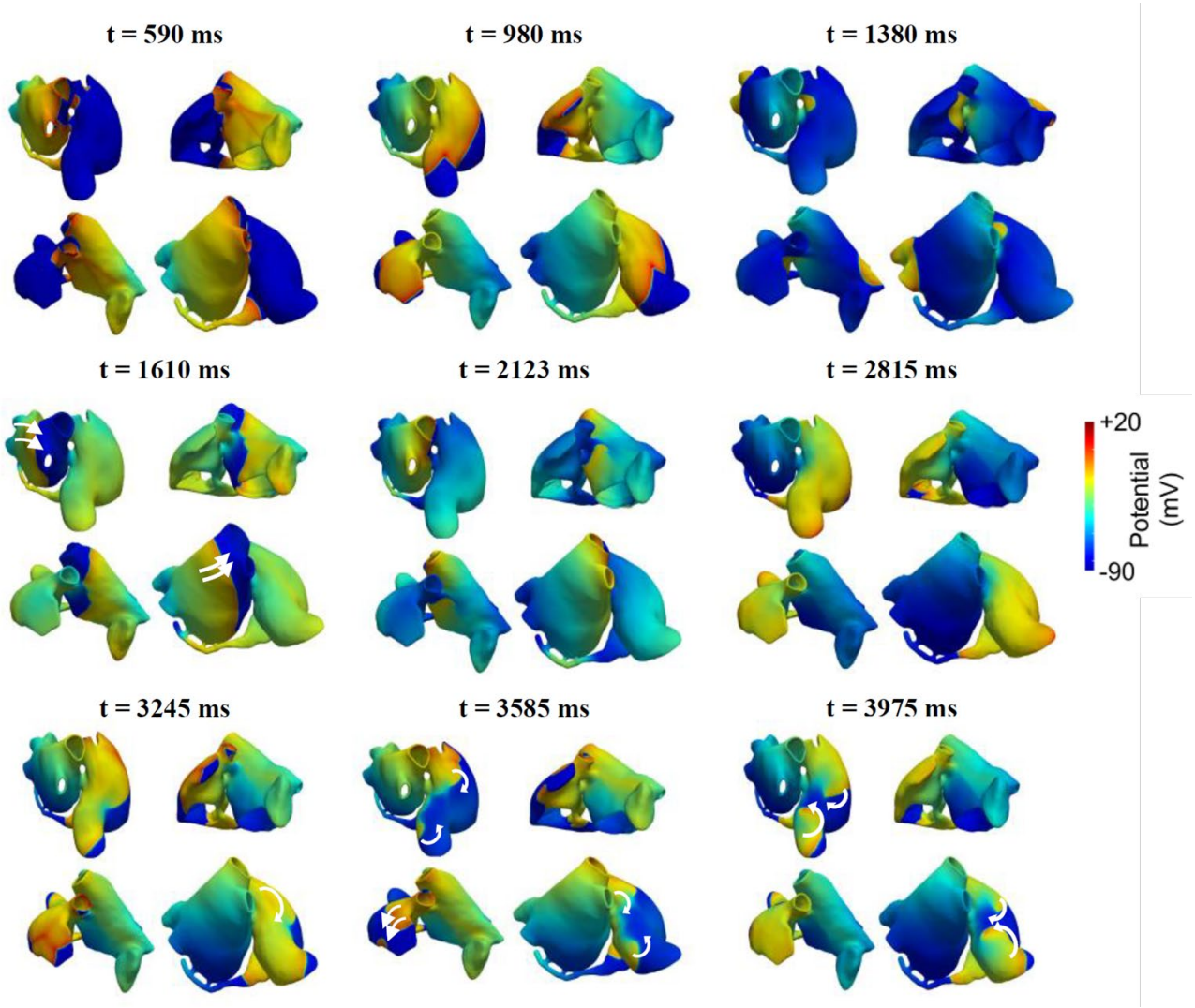

Figure S6 – Snapshot of scroll waves for the mutation KCNH2 T895M Snapshot of spiral wave activity observed in the 3D patient-specific atrial model in presence of the mutation KCNNH2 T895M. The arrhythmic pattern was evoked by stimulating the EF located in the middle of the LPVs, with a BCL equal to 160 ms and with a coupling interval equal to 180 ms. White arrows indicate the direction of the propagating waves.

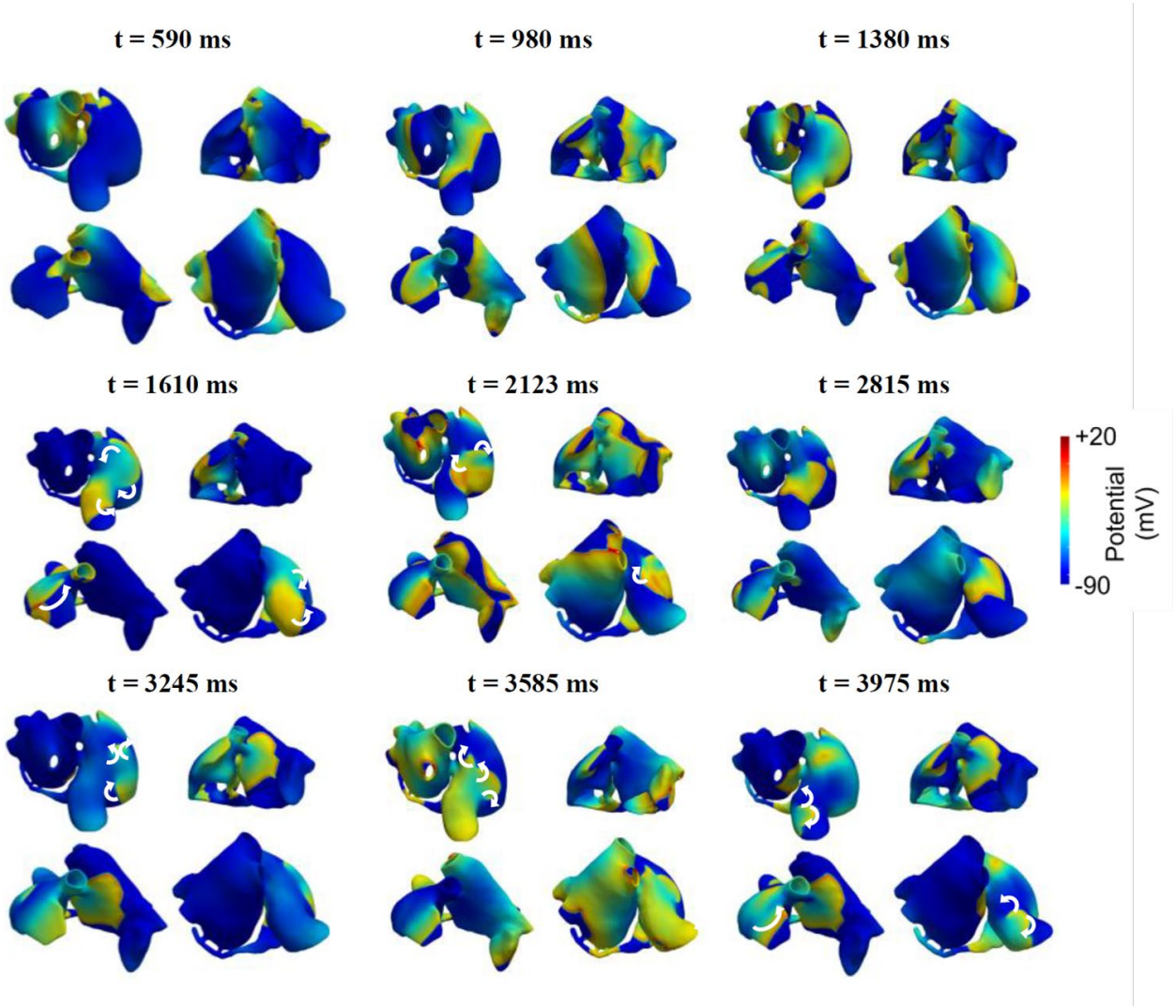

Figure S7 – Snapshot of scroll waves for the mutation KCNE3-V17M. Snapshot of spiral wave activity observed in the 3D patient-specific atrial model in presence of the mutation KCNE3-V17M. The arrhythmic pattern was evoked by stimulating the EF located in the middle of the LPVs, with a BCL equal to 100 ms and with a coupling interval equal to 20 ms. White arrows indicate the direction of propagation.

Bibliography

[1] A. Ferrer *et al.*, “Detailed anatomical and electrophysiological models of human atria and torso for the simulation of atrial activation,” *PLoS One*, vol. 10, no. 11, pp. 1–29, 2015, doi: 10.1371/journal.pone.0141573.

[2] M. W. Krueger *et al.*, “Modeling atrial fiber orientation in patient-specific geometries: A semi-automatic rule-based approach,” *Lect. Notes Comput. Sci. (including Subser. Lect. Notes Artif. Intell. Lect. Notes Bioinformatics)*, vol. 6666 LNCS, pp. 223–232, 2011, doi: 10.1007/978-3-642-21028-0_28.

[3] R. Lemery *et al.*, “Normal atrial activation and voltage during sinus rhythm in the human heart: An endocardial and epicardial mapping study in patients with a history of atrial fibrillation,” *J. Cardiovasc. Electrophysiol.*, vol. 18, no. 4, pp. 402–408, 2007, doi: 10.1111/j.1540-8167.2007.00762.x.